LANGMUIR Article
Cite This: Langmuir 2018, 34, 4398−4407
pubs.acs.org/Langmuir

Membrane Restructuring Events during the Enzymatic Generation of Ceramides with Very Long-Chain Polyunsaturated Fatty Acids

Daniel A. Peñalva,*[,†,‡] Silvia S. Antollini,[†,‡] Ernesto E. Ambroggio,[§,∥] Marta I. Aveldaño,[†,‡] and María L. Fanani[§,∥]

[†]Instituto de Investigaciones Bioquímicas de Bahía Blanca, Consejo Nacional de Investigaciones Científicas y Técnicas (CONICET) and Universidad Nacional del Sur (UNS), 8000 Bahía Blanca, Argentina

[‡]Departamento de Biología, Bioquímica y Farmacia, UNS, 8000 Bahía Blanca, Argentina

[§]Centro de Investigaciones en Química Biológica de Córdoba, CONICET−Universidad Nacional de Córdoba (UNC), 5000 Córdoba, Argentina

[∥]Departamento de Química Biológica "Ranwel Caputto", Facultad de Ciencias Químicas UNC, 5000 Córdoba, Argentina

Supporting Information

ABSTRACT: In rat sperm heads, sphingomyelin (SM) species that contain very long-chain polyunsaturated fatty acid (V-SM) become ceramides (V-Cer) after inducing in vitro the acrosomal reaction. The reason for such a specific location of this conversion, catalyzed by a sphingomyelinase (SMase), has received little investigation so far. Here, the effects of SMase were compared in unilamellar vesicles (large unilamellar vesicles (LUVs), giant unilamellar vesicles (GUVs)) containing phosphatidylcholine, and either V-SM or a palmitate-rich SM (P-SM). In uniformly sized LUVs at 37 °C, more V-Cer was generated and more rapidly than P-Cer. Nephelometry and dynamic light scattering showed that LUVs tended to form large lipid particles more intensely, and Förster resonance energy transfer (FRET) increases suggested that lateral lipid mixing was more marked when V-Cer rather than P-Cer was produced. As reported by 6-dodecanoyl-2-dimethyl-aminopnaphthalene (Laurdan) and 1,6-diphenyl-1,3,5,-hexatriene (DPH), the production of V-Cer resulted in higher and faster restriction in lipid mobility than that of P-Cer, implying a stronger increase in membrane dehydration and microviscosity. Moreover, DPH anisotropy suggested a higher solubility of V-Cer than that of P-Cer in the liquid-disordered phase. At room temperature, liquid-condensed lateral domains appeared in P-SM- but not in V-SM-containing GUVs. The former maintained their size while losing their contents gradually during SMase action, whereas the latter became permeable earlier and reduced their size in few minutes until suddenly collapsing. The fast and potent generation of V-Cer may contribute to the membrane restructuring events that occur on the acrosome-reacted sperm head.

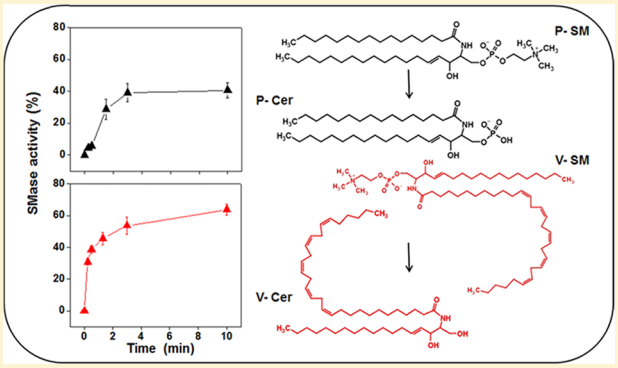

INTRODUCTION

The sphingolipids of most mammalian tissues typically contain saturated (16:0, 18:0, and 24:0) and monounsaturated (18:1, 22:1, and 24:1) fatty acids. A notable exception is the mammalian germ cells and spermatozoa, which contain sphingomyelin (SM)[1] and ceramide (Cer) species[2] with very long-chain polyunsaturated fatty acids (VLCPUFA). These amide-bound acyl chains contain 26−36 carbon atoms and 4, 5, or 6 double bonds, the length and unsaturation varying according to the species. In germ cells from adult rodents, part of the VLCPUFA of sphingolipids contain a 2-hydroxyl group at the second carbon atom of their fatty acyl chain, as previously shown for SM,[3] a specific series of gangliosides,[4] and Cer.[5] In the rat testis, nonhydroxy-VLCPUFA are almost exclusive components of the SM and Cer from precursor spermatocytes, whereas the proportion of species containing a 2-hydroxy VLCPUFA increases as these cells differentiate into spermatids and the latter into spermatozoa.[6] In mature gametes, the distribution of the species of SM between head and tail is uneven.[7] Thus, relatively high percentages of virtually only VLCPUFA-containing SM species (V-SM) abound in sperm heads, whereas the sperm tails lack such SM species, their SM being instead rich in palmitic acid (P-SM). In rat spermatozoa, almost complete hydrolysis of the head-located V-SM into V-Cer by an endogenous sphingomyelinase (SMase) occurs after inducing the acrosomal reaction in vitro by means of a calcium ionophore (A23187).[8]

Received: December 28, 2017
Revised: February 14, 2018
Published: March 15, 2018

DOI: 10.1021/acs.langmuir.7b04374
Langmuir 2018, 34, 4398−4407

Some biophysical properties of the major SM species that contain nonhydroxy and 2-hydroxy versions of 28:4, 30:5, and 32:5 in bilayers[9] and in Langmuir monolayers[10] have been previously reported by our group. Both in bilayer and monolayer studies, the differences among V-SM species due to chain length and unsaturation of their acyl groups and also those associated to the presence versus absence of the 2-hydroxyl group, albeit significant, were relatively small in comparison with the ample differences any of these species displayed with the archetypical saturated or monounsaturated species of SM.[10] In large unilamellar vesicles (LUVs) containing binary mixtures of dimiristoylphosphatidylcholine and V-SM or palmitoyl-SM (P-SM), the former decreased, whereas the latter increased the transition temperature of the glycerophospholipid. In giant unilamellar vesicles (GUVs) containing 1-palmitoyl-2-oleoylphosphatidylcholine (POPC), cholesterol (Chol), and V-SM, the latter did not separate into SM/cholesterol-rich lateral domains as P-SM typically does.[9]

In 6-dodecanoyl-2-dimethyl-aminopnaphthalene (Laurdan)-labeled LUVs prepared with the total membrane phospholipid components from rat spermatozoa and cholesterol, the experimental addition of increasing amounts of the Cer species obtained from acrosome-reacted sperm augmented the membrane generalized polarization (GP) values.[8] The facts that V-SM species are exclusive components of the sperm head[7] and that they may be readily converted into V-Cer prompt the question of what is the reason for such a specific location of these sphingolipids, interconnected by the action of a sperm-associated SMase. The answer to this question remains unknown because it has received limited investigation.

The present study started with the hypothesis that some clues may be gained from examination of what happens physically in membrane models during the V-SM → V-Cer enzymatic conversion, used to compare the widely studied P-SM → P-Cer reaction.[11−13] Key properties of uniformly sized vesicles composed of POPC and SM, with the SM of such mixture being either V-SM or P-SM, were comparatively examined before, during, and after exposures to SMase. This model strived for minimalism in order to make the comparisons as neat and simple as possible, not including lipids that have been shown to have their own and specific influence during the SM → Cer conversion. This is the case for instance when, in addition to POPC and P-SM, the vesicles exposed to SMase contain cholesterol (Chol)[14] or phosphatididylethanolamine (PE).[15,16]

The present results show that the enzymatic production of V-Cer from V-SM induces alterations to the properties and structure of SMase-treated vesicles that are clearly different from those that occur when P-Cer is produced from P-SM. This includes changes in vesicle size, permeability, and stability that could be relevant to the changes that occur on the sperm head during AR-associated functions.

EXPERIMENTAL SECTION

Materials. The SM species with very long-chain PUFA (V-SM) used in this study were obtained from adult Wistar rat testes.[9] Briefly, the total SM was isolated from total lipid extracts by thin-layer chromatography (TLC), eluted, purified by exposure to mild alkali, and subjected to argentation TLC to recover the V-SM species. The latter were further subjected to TLC on silica gel H to separate them into species containing nonhydroxy- and 2-hydroxy-VLCPUFA. The latter, mostly containing 2-hydroxy-derivatives of 30:5 n-6,[9] was the fraction used in this study. To protect the polyunsaturated lipid samples from oxidation, all isolation steps and experimental manipulations were carried out under nitrogen. The purity of the samples after isolation was checked by high-performance liquid chromatography (HPLC).[9] As a control for comparison, we used egg SM, here abbreviated P-SM because palmitatate (P) represents 95% of its fatty acids. This P-SM, 1-palmitoyl-2-oleoylphosphatidylcholine (POPC), and the fluorescent probes L-α-phosphatidylethanolamine-*N*-(lissaminerhodamine B sulfonyl) (Rho-PE) and L-α-phosphatidylethanolamine-*N*-(7-nitro-2-1,3-benzoxadiazol-4-yl) (NBD-PE), ammonium salts, were from Avanti Polar Lipids, Inc. (Alabaster, AL). 6-Dodecanoyl-2-dimethyl-aminopnaphthalene (Laurdan) and 1,6-diphenyl-1,3,5,-hexatriene (DPH) were from Invitrogen (Eugene, Oregon). Alexa^{488}, BODIPY-ceramide, bovine milk β-casein, and SMase (from *Bacillus cereus*) (EC 3.1.4.12) were from Sigma-Aldrich (St. Louis, MO). All solvents used were HPLC grade (Merck, Darmstadt, Germany). Deionized water, with a resistivity of 18 MΩ cm, was obtained from a Milli-Q Gradient System (Millipore, Bedford, MA). The indium tin-oxide (ITO) slides were obtained from Nanocs (New York).

METHODS

Vesicle Preparation. Multilamellar vesicles containing binary POPC/P-SM or POPC/V-SM mixtures were obtained from lipid solutions. The preparations were placed for 1 h in the dark under a constant flow of N_2 for solvent evaporation. The dried lipid films were hydrated with a buffer solution (10 mM *N*-(2-hydroxyethyl)-piperazine-*N*′-ethanesulfonic acid (HEPES), 200 mM NaCl, 10 mM $CaCl_2$, 2 mM $MgCl_2$, pH 7.0), mixed vigorously, and subjected to five freezing−thawing cycles (−195 and 40 °C, respectively). Large unilamellar vesicles (LUVs) with an average diameter of 100 nm were obtained by subjecting these vesicles to extrusion (20 times) through polycarbonate filters of 100 nm pore size, at room temperature. Vesicles were prepared either in unlabeled form or labeled with fluorescent probes with fluorescent probes (e.g., Laurdan, DPH, Rho-PE, NBD-PE). In this case, small aliquots of the probe solutions to reach a lipid/probe molar ratio of 100:1 or lower were added to the lipid mixtures to obtain the labeled vesicles required in each case.

Enzymatic Activity. Unlabeled LUVs containing POPC and either P-SM or V-SM, in the same PC/SM molar ratio (3:1) and diluted to reach a 150 μM total lipid concentration, were incubated with *Bacillus cereus* SMase (1.4 U/mL) at 37 °C. Aliquots of this suspension were taken at regular intervals and the solvents methanol and chloroform were added. The lipids were extracted, the solvents evaporated, and the samples subjected to TLC. Chloroform/methanol/acetic acid/water (50:37.5:3.5:2, v/v/v/v) was run up to approximately the middle of the plates to separate PC from SM, and, after drying the plates, hexane/ether (80:20, v/v) was run up to the top of the plates to isolate the ceramides. For lipid location and quantification, the plates were sprayed with an aqueous solution of 3% p/v cupric acetate−8% v/v phosphoric acid and heated (see for example Figure 1A). Lipid semiquantification was performed using the ImageJ 1.43u programme (NIH).

Effects of SMase on Vesicle Size. Nephelometry and vesicle size distribution data were obtained using unlabeled LUV preparations containing POPC and either P-SM or V-SM, as just described (3:1 molar ratio, 1.4 U/mL enzyme, 37 °C), immediately before (t = 0), during, and at specified incubation times with SMase. To optimize measurements, an amount of vesicles corresponding to a lipid concentration of 500 μM instead of 150 μM was used for nephelometry. The intensity of the scattered light was measured at 90° from the incident beam (λ = 530 nm) using a Cary Eclipse fluorescence spectrophotometer (Varian Medical Systems, Inc., Palo Alto, CA). The change in light scattering as a function of incubation time was determined for each vesicle type by comparing the values of light scattering at a given time t_t with respect to t_o.

Changes in vesicle size distribution profiles as a consequence of SMase action were followed using dynamic light scattering (DLS) using a Submicron Particle Sizer (Nicomp 380, Santa Barbara, CA). Starting in each case from the 100 nm LUV preparations to be

DOI: 10.1021/acs.langmuir.7b04374
Langmuir 2018, 34, 4398−4407

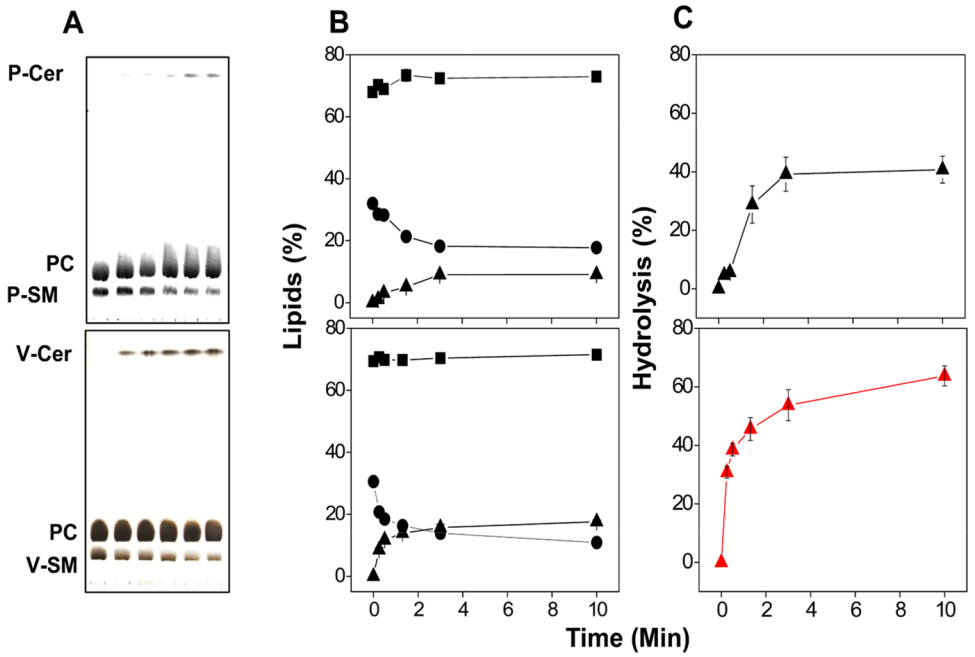

Figure 1. Time course of the SMase-driven conversion of sphingomyelin (SM) to ceramide (Cer) in liposomes containing either V-SM or P-SM. LUVs composed of PC/SM (3:1 molar ratio), with PC being POPC and SM being either P-SM (palmitate-rich egg SM) or V-SM (VLCPUFA-rich SM species from rat testis) were suspended in buffer (total lipid concentration in the suspensions, 150 μM). The enzyme (1.4 units/mL) was added at t = 0, incubations proceeded at 37 °C for the indicated intervals, and the activity was stopped by addition of the solvents required for lipid extraction. (A) Representative TLC separations at comparable intervals. (B) Semiquantitative profiles showing the percentages of the three lipids in the system: POPC (squares), SM (circles), and Cer (triangles). (C) Percentage of the SM present at t = 0 that was converted into Cer. Data in (B) and (C) are mean values ± standard error of the mean (SEM) from three independent experiments (n = 3).

compared, the particle size distribution tracings at the same incubation time with SMase were obtained. The percentage with respect to the total volume occupied by the population of lipid particles larger than 150 nm was calculated from the areas under the peaks in the corresponding size distribution tracings.

Laurdan Generalized Polarization (GP) and DPH Fluorescence Anisotropy (r). To follow the changes in the Laurdan GP and DPH r values with SMase action, each of the probes was included in the POPC/SM vesicles under study (100 nm particle size, lipid/probe ratio of 100:1). The enzyme was added at t = 0, and incubation proceeded as described for unlabeled vesicles. Laurdan-labeled vesicle suspensions were subjected to an excitation wavelength of 360 nm, and the intensity of the fluorescence emitted at 434 and 490 nm (I_{434} and I_{490}, respectively) was recorded. Laurdan GP values were calculated according to the expression

$$\mathrm{GP} = \frac{(I_{434} - I_{490})}{(I_{434} + I_{490})} \quad (1)$$

When Laurdan is present in phospholipid bilayers, the intensities I_{434} and I_{490} are known to be proportional to the fraction of the lipid molecules that adopt a gel phase and a liquid-crystalline phase, respectively.[17] From eq 1, it follows that increases in GP values denote higher structural lipid order.

The excitation and emission wavelengths for DPH-labeled vesicles were 365 and 425 nm, respectively. The fluorescence anisotropy was measured in the T format with Schott KV418 filters in the emission channels and corrected for optical distortions and background signals. The DPH fluorescence anisotropy values, r, were obtained from the equation

$$r = \left(\frac{I_v}{I_h}\right)_v - \left(\frac{I_v}{I_h}\right)_h \Big/ \left(\frac{I_v}{I_h}\right)_v + 2\left(\frac{I_v}{I_h}\right)_h \quad (2)$$

associating the ratios of the intensities of the polarized light (l) emitted vertically (v) or horizontally (h) versus the exciting vertical or horizontal polarized light, respectively.[18] The DPH anisotropy measures the movement of the probe in the hydrophobic environment of the membrane lipid hydrocarbon chains. Thus, increases in r values denote higher microviscosity and hence, indirectly, a higher structural lipid order.

Vesicle Mixing Assays. Membrane reordering and lipid lateral mixing after treatment with SMase was estimated by analyzing the increase in the Förster resonance energy transfer (FRET)[19] in the vesicles under study. For this purpose, two POPC/P-SM and two POPC/V-SM vesicle populations were prepared: in each case, one contained 0.6 mol % of NBD-PE (donor) and the other contained 0.6 mol % of Rho-PE (acceptor). Equivalent liposome populations containing each of these probes were mixed in a 1:1 ratio, SMase was added, and incubations proceeded for similar intervals. The donor was excited at 450 nm, and its fluorescence intensity emission (520 nm) was recorded before (t = 0) and after comparable incubation times ($t = t_t$) with the enzyme. Membrane reordering and lipid lateral mixing was estimated from the relative decrease of the donor emission using the expression

$$100 \times \left(1 - \frac{F\ \text{donor}}{F_0\ \text{donor}}\right) \quad (3)$$

where F_0 and F are the values of the fluorescence emission of the donor at t = 0 and $t = t_t$, respectively.

All fluorimetric measurements were performed in an SLM model 4800 fluorimeter (SLM Instruments, Urbana, IL) using the vertically polarized light beam from a Hannovia 200 W Hg/Xe arc obtained with a Glan-Thompson polarizer (4 nm excitation and emission slits) and 5 × 5 mm^2 quartz cuvettes. Emission spectra were corrected for wavelength-dependent distortions. The liposomes were allowed to equilibrate for 10 min at the reaction temperature, which was set with a circulating water bath.

Membrane Restructuring in SMase-Treated GUVs. GUVs containing POPC and either P-SM or V-SM, in a 3:1 mole ratio, were prepared to contain simultaneously two fluorescent molecules, the hydrophobic BODIPY-Cer and the water-soluble Alexa^{488}, to mark the

DOI: 10.1021/acs.langmuir.7b04374
Langmuir 2018, 34, 4398−4407

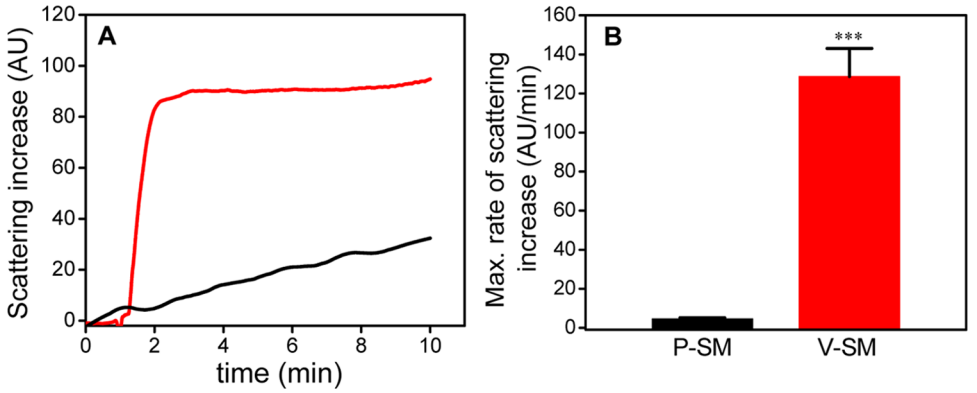

Figure 2. Differences in light scattered by lipid particle suspension resulting from the enzymatic conversion of P-SM or V-SM to the corresponding ceramides. LUVs (100 nm diameter) composed of POPC and each of the indicated SM (3:1 molar ratio) were exposed to SMase (1.4 units/mL) at t = 0, and incubations proceeded at 37 °C, as described in Figure 1. The light scattered at 90° from the incident beam (λ = 530 nm) was recorded as a function of time in comparison with that at t = 0 min. (A) Vesicles initially containing either P-SM (black line) or V-SM (red line). (B) Mean values of the maximum rates of increase in scattering ± SEM (n = 3).

GUV membrane and aqueous contents, respectively. Both GUV populations were prepared by the electroformation method.[20] Briefly, from lipid solutions containing each of the PC/SM mixtures under study (0.5 mg/mL in chloroform/methanol), 10 μL was taken, doped with 0.2 mol % of BODIPY-Cer, and spread onto one ITO-coated glass slide. The electrode was subjected to vacuum to remove traces of the organic solvents. The dried lipids were then hydrated with a solution of sucrose (269 mM) doped with 0.2 mol % Alexa^{488}, and the electrodes were connected to a function generator (UNI-T UTG9002C, Uni-Trend Group Limited, Hong Kong). A low-frequency alternating field (sinusoidal function of 10 Hz and an effective tension of 1 V)[21] was then applied for 5 h.

A small aliquot of the GUV suspensions (20 μL) was transferred onto an 8-well observation chamber (Lab-Tek, Thermo Fisher Scientific, Inc., NYSE:TMO) containing an iso-osmotic buffer solution. Before GUV additions into the well, the glass of the observation chamber was treated with a 10 mg/mL β-casein solution to prevent GUV rupture onto the slide. The GUVs were directly observed in a fluorescence confocal microscope (Olympus FV 300, Tokyo, Japan) before (t = 0) and at specific times after SMase addition. Time-lapsed images (3 s between frames) of the GUVs were acquired at room temperature, starting immediately after the enzyme was added and following the fluorescence of BODIPY-Cer and of Alexa^{488}, in the red and green channel, respectively. Changes in the fluorescence intensity in both channels were quantified with the ImageJ 1.43u software (NIH).

Data Analysis. Intergroup comparisons were carried out using the paired Student's t-test Intergroup with the values representing the average ± SEM of the total number of samples indicated in each figure legend as follows: *, statistically significant (p < 0.05) and **, ***, statistically very significant differences (p < 0.01 and p < 0.001, respectively).

RESULTS AND DISCUSSION

Enzymatic SM → Cer Conversion. A comparison of the effects of SMase on the generation of Cer from LUVs containing POPC and either P-SM or V-SM is shown in Figure 1. In the presence of an unchanged amount of POPC, an increase in the level of Cer and a concomitant decrease in that of SM were evident as the reaction time elapsed (Figure 1A,B). Whereas the vesicles initially containing P-SM underwent a maximum degree of hydrolysis plateauing at nearly 40% in 3 min (no difference between 3 and 10 min), those containing V-SM displayed 50 and 60% hydrolysis at 3 and 10 min, respectively, with no plateau reached in the interval under study (Figure 1C). Given the simplicity of the present two-lipid systems and assuming that the SMs would be located symmetrically between both hemilayers of the vesicle bilayers, we initially expected that although at different incubation times, the maximum substrate conversion should be close to 50% for both SM species. The inequality observed in Figure 1 suggests that the enzyme hydrolyzes mostly SM molecules located in the outer hemilayer of the vesicle bilayers only when the substrate was P-SM, whereas it was able to reach part of those located in the inner hemilayer when it was V-SM. The percentage of hydrolysis in the control POPC/P-SM binary system at 37 °C agreed with that in previous data obtained at room temperature.[14] The maximal degree of SMase-induced hydrolysis was slightly lower (30−35%), as expected, but the trend to rapidly plateau and to persist unchanged for long periods at the same percentage was similar. Notably, the authors showed that this hydrolysis increases (to as much as ∼65−70%) when the bilayer is restructured by the presence of high concentrations of Chol.[14] It was then remarkable that the present POPC/V-SM system reached more than 50% of V-SM hydrolysis in few minutes in the total absence of Chol.

It must be borne in mind that SMase activity critically depends on the phase state of its SM substrate.[22] However, despite the T_m of P-SM (42 °C) being far higher than that of V-SM (below 0 °C),[9] when mixed with POPC as the predominant lipid (3:1 molar ratio) at 37 °C, P-SM[23] and V-SM[9] produce bilayers in the liquid-disordered phase. Thus, the dissimilarities observed are not caused by differences in enzyme accessibility to each of its substrates.

The initial velocity of the reaction, estimated at short intervals (≤1.5 min), was lower for P-SM than for V-SM, giving values estimated in 12 ± 3 × 10^{-3} and 54 ± 9 × 10^{-3} μmol/min, respectively. That these differences are due to a higher affinity of *B. cereus* SMase toward V-SM than toward P-SM may be disregarded, as the enzyme only recognizes the phosphocholine headgroup. The fact that the generation of P-Cer tends to limit, whereas that of V-Cer facilitates the access of SMase to the SM molecules originally present in both hemilayers, suggests that the bilayer reorganizes in different ways in each case.

Enzymatically Induced Formation of Large Lipid Particles and Lipid Mixing. Previous data had shown that the addition of SMase to liposomes of pure P-SM and to mixtures of PC with P-SM progresses, with time, with an

DOI: 10.1021/acs.langmuir.7b04374
Langmuir 2018, 34, 4398−4407

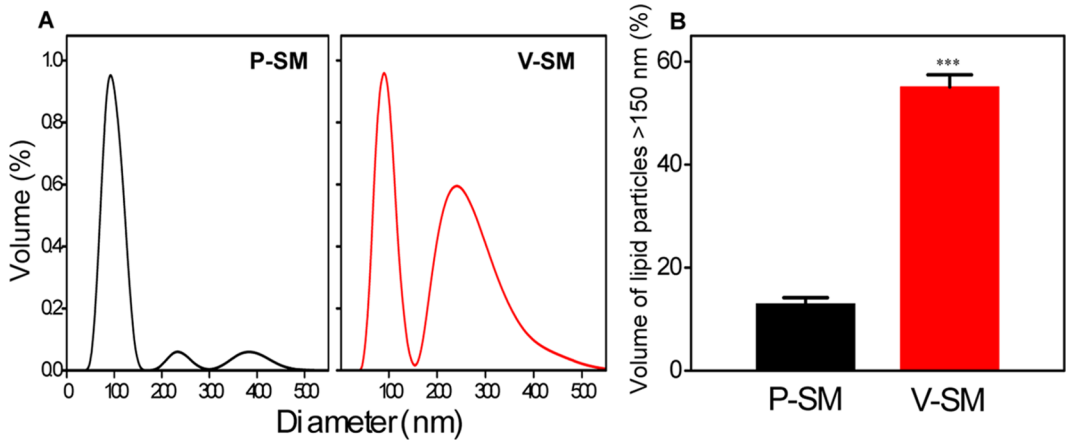

Figure 3. Lipid particle size differences after SMase action from LUVs initially containing V-SM or P-SM. LUVs (100 nm diameter) LUVs, prepared with POPC, and each of the indicated SM species (3:1 molar ratio) were exposed to SMase (1.4 units/mL) at 37 °C and incubated for 15 min. Immediately, next, the particle size distribution was determined by dynamic light scattering (DLS). (A) Comparison of the profiles of vesicle size distribution between LUVs initially containing P-SM or V-SM. (B) Percentage of the volume of lipid particles, with respect to the total, that were larger than 150 nm, calculated from the size distribution tracings shown in (A). Mean values ± SEM (n = 3).

increase in turbidity.[22] This was confirmed in the present study by the significant increase in the amount of light scattered at 90° when SMase was added to LUVs containing the same (3:1) molar ratios between POPC and either P-SM or V-SM (Figure 2). Compared with LUVs containing P-SM, the amount of light scattered by lipid particle suspensions composed of V-SM not only had increased more (5-fold higher) (Figure 2A) but also had a higher maximum rate of scattering increase (Figure 2B), reaching a maximum value more rapidly (within 2−3 min).

Starting from a vesicle size population of 100 nm, the fact that they tend to form larger lipid particles after SMase action was confirmed by following the changes induced to the particle size distribution tracings using dynamic light scattering analysis (DLS) (Figure 3). In the absence of SMase, the LUVs of pure POPC used as controls, as those of the two POPC/SM systems under study, showed a nearly monodisperse population of vesicles, with a bell-shaped curve centered at 100 nm in particle diameter (not shown). The enzymatic hydrolysis of SM induced polydispersion in the distribution of particles that contained either P-SM or V-SM. Remarkably, when P-Cer was generated, only about 15% of the particle population was organized in structures with a diameter larger than 150 mm, in contrast to as much as 45% of the vesicles when the enzymatic product was V-Cer (Figure 3).

The SMase-induced increase in lipid particle size shown in Figures 2 and 3 evidence vesicle restructuring into larger lipid structures. Although the mechanisms involved in such size increase were not determined in the present study, that lipid mixing was taking place during these size changes was suggested by the results of FRET experiments (Figure 4). Liposomes containing POPC and either P-SM or V-SM were prepared similarly except that one part of each contained the FRET donor NBD-PE and the other one contained the FRET acceptor Rho-PE. Vesicles of the same size containing the same SM and each of the probes in their membranes were mixed at a 1:1 lipid molar ratio. In the absence of SMase, the FRET process exhibited by the Rho-PE donor emission, revealed by a shoulder in the spectrum at λ = 583 nm, was significantly more pronounced for the vesicles containing V-SM than for those containing P-SM (Figure 4A). Associated to SMase-driven Cer formation, an important drop in the emission of the donor was observed in both cases. However, such a decrease was much faster (Figure 4B-I) and quantitatively more prominent (3-fold, Figure 4B-II) when V-Cer, rather than P-Cer, was the lipid product. The increases in FRET support the conclusion that the occurrence of larger lipid particles observed by nephelometry and DLS involves lateral lipid mixing and membrane recombination.

Membrane Surface Hydration and Microviscosity. The time course of the effect of P-Cer or V-Cer enrichment on the membrane properties was followed by taking advantage of the fluorescent properties of Laurdan, a dye that is sensitive to the hydration of the lipid interface,[24,25] and DPH, which allows to indirectly monitor the degree of lipid mobility or rigidity in the deeper hydrophobic environment of the membranes.[26] Because Laurdan spontaneously locates at the level of the polar layer of phospholipids in membranes, its fluorescence is known to be strongly influenced by the dipolar relaxation of the water molecules in this region. In the present study, the generalized polarization (GP) values of this probe increased substantially with the SM → Cer conversion when either P-SM or V-SM was the SMase substrate (Figure 5A). This evidenced that with respect to the initial situation, the presence of Cer molecules changed the presence or amount of water molecules at the membrane surface level, interfering with the dipolar relaxation of the excited Laurdan molecules. Although this effect took place during SMase action in both cases, it was significantly stronger for the V-SM/V-Cer than for the P-SM/P-Cer system, denoting a greater increase of the lipid structural order with respect to t = 0 in the former case.

An increase in the DPH anisotropy (r) values in a membrane as a reaction progresses denotes an increase in the membrane microviscosity. Associated to the activity of SMase, an increase in r was observed with both LUVs being compared (Figure 5B). For the POPC/P-SM (3:1) system, this increase was essentially similar to that previously described by Holopainen et al.[27] The fact that the r values increased with P-Cer or V-Cer generation is consistent with the acyl chains of both Cer restraining the initially high mobility of the lipids in the membrane matrix. It must be borne in mind that DPH is excluded from rigid Cer-enriched gel domains[28,29] for it only reports the microviscosity sensed in the fluid phase. Remarkably, the Cer concentration-dependent increase in mobility restriction was twice higher

DOI: 10.1021/acs.langmuir.7b04374
Langmuir 2018, 34, 4398−4407

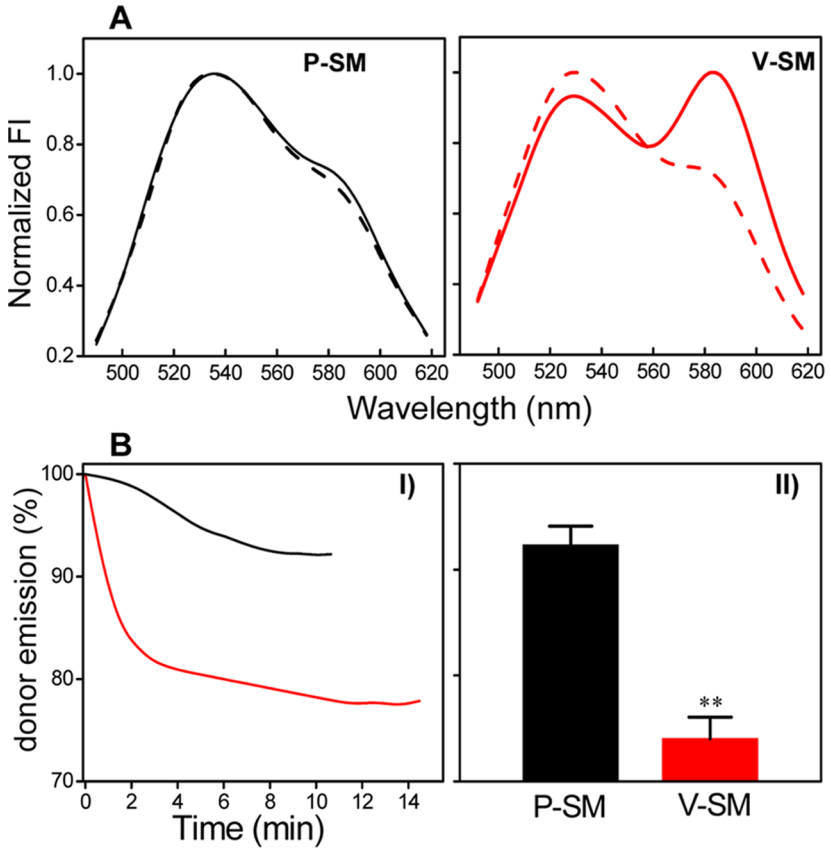

Figure 4. Membrane mixing associated with SMase activity in LUVs initially containing either P-SM or V-SM. Two populations of Luvs (100 nm diameter), composed of POPC and each of the indicated SM species (3:1 molar ratio), were prepared, one to contain the FRET donor NBD-PE and the other to contain the FRET acceptor Rho-PE. Donor- and acceptor-labeled vesicles containing the same SM were mixed at a 1:1 molar ratio, exposed at t = 0 to SMase (1.4 units/mL), and incubated at 37 °C for comparable intervals. (A) Fluorescence intensity spectra, taken immediately before (dash lines) and 10 min after (full lines) the addition of SMase, superimposed for comparison. (B-I) Time course of the decrease in emission intensity of the donor NBD-PE when it was initially present in vesicles containing P-SM (black line) or V-SM (red line). Data were calculated using eq 3, as described in Methods. (B-II) Percentages of the donor emission intensity at t = 10 min (mean values ± SEM, with n = 3).

when V-Cer rather than P-Cer was the SMase product (Figure 5B).

Previous studies had shown that h-28:4 Cer mixes more favorably with h-28:4 SM than P-Cer with P-SM, the former segregating into Cer-enriched domains only after reaching a Cer/SM ratio of 25 mol %, in contrast to the typical 5−7 mol % P-Cer required by the latter binary mixture.[30] Then, it may be expected that more of the V-Cer than the P-Cer molecules produced by SMase remain dispersed in the liquid phase provided by the POPC-rich environment, reaching higher concentrations there. This may respond to the larger increase in the microviscosity detected by DPH when V-Cer was the product, rather than P-Cer.

In addition to the higher solubility of V-Cer than that of P-Cer in the liquid-disordered POPC phase, these ceramide species greatly differ in their rheological properties when they are in their liquid-condensed state, as observed by Brewster angle microscopy in Langmuir monolayers at room temperature.[10] In contrast with the highly rigid condensed P-Cer domains,[31] the liquid-condensed V-Cer domains are characterized by the presence of a thick and soft compressible phase, a property that is compatible with the highly disordered conformation of the bulky fatty acid chain of this Cer. At the same time, such phase is highly restrictive to the lateral diffusion of molecules within these domains, as shown by single particle tracking.[30] These distinctive features are consistent with the higher increases in GP and r values during V-Cer, rather than P-Cer, generation.

Membrane Stability. The structural membrane reorganization after SMase treatment was followed as a function of time by direct visualization through confocal fluorescence microscopy. GUVs containing POPC and the P-SM or V-SM species being compared (3:1) were doubly labeled with a lipophilic and a water-soluble fluorescent probe to mark the membrane and the fluid compartment enclosed, respectively. In the absence of enzyme (t = 0), the GUVs containing P-SM displayed inhomogeneity in membrane fluorescence. In different sections of the GUV spheres, darker zones on the bright red-labeled bilayer were observed (Figure 6A). As this P-SM is the only high-melting component of this simple binary lipid bilayer, this is evidence that a fraction of the P-SM molecules was forming part of an SM-enriched domain in the gel phase. This is consistent with the known fact that at room temperature, P-SM in the gel phase and POPC in the liquid phase can coexist in the plane of a vesicle bilayer.[23] As these GUVs were treated with SMase, the originally dark membrane regions became progressively interspersed with small red-labeled regions (Figure 6A). This is consistent with the enzyme decreasing the size of the original P-SM platforms and forming smaller P-Cer domains, surrounded by fluid POPC-enriched phase, as suggested by the bright red spots observed within the

DOI: 10.1021/acs.langmuir.7b04374
Langmuir 2018, 34, 4398−4407

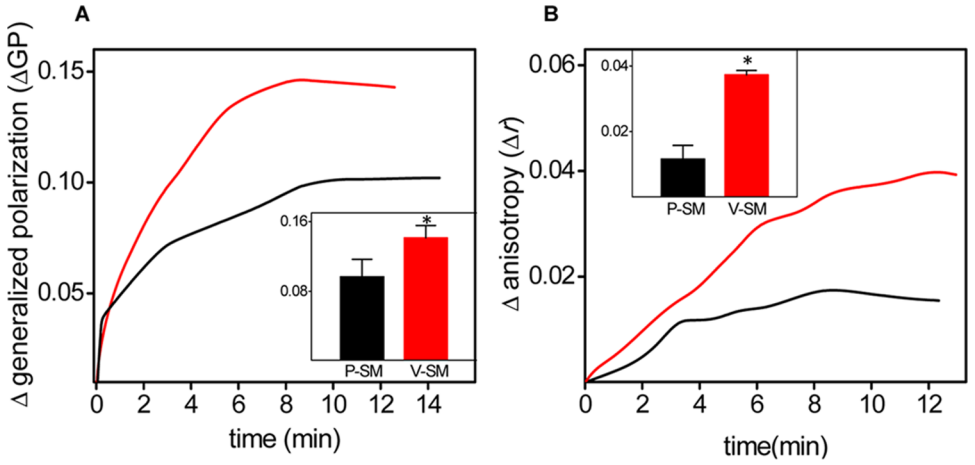

Figure 5. Laurdan generalized polarization (A) and DPH anisotropy (B) during SMase activity. LUVs of (100 nm diameter) containing POPC and either P-SM or V-SM, at a 1:1 molar ratio (150 μM total lipid concentration), doped with 1% of Laurdan or DPH, were warmed to 37 °C. The enzyme (1.4 units/mL) was added at t = 0, and incubations proceeded for similar intervals. Differences (Δ) with respect to t = 0 were recorded for P-SM (black lines) and V-SM (red lines). Bars showing the mean values ± SEM (with n = 3) of the data of each figure at t = 10 min in each case.

dark regions (Figure 6A, with detail shown, in amplified form, in Supporting Information Section S2).

When V-SM was the component of the GUV POPC/SM mixture, a completely different picture emerged. There was no evidence of laterally segregated gel domains, indicating that V-SM does not segregate as P-SM does. Thus, at t = 0, in comparable conditions of vesicle size, PC/SM ratio, and temperature as P-SM, the V-SM molecules mixed freely with the POPC molecules present in the fluid matrix. During SMase action, even when some minutes had elapsed and an important amount of V-Cer was generated, separate Cer domains were not apparent (Figure 6A).

A common characteristic of the P-SM- and V-SM-containing GUVs was that both became permeable due to SMase action, eventually losing most of their green fluorescent contents. The green fluorescence originally present in the inner aqueous compartment disappeared gradually from the P-SM containing GUVs. Thus, more than half the original contents was retained in the vesicles at t = 240 s (Figure 6B). In comparison, when V-SM was the substrate of SMase, the efflux of the green fluorescent marker from the vesicles was rapid and massive, being almost complete at t = 240 s. P-SM-containing vesicles preserved their shape and size while releasing their contents (Figure 6C). The vesicle contours persisted even when they have lost all the internal fluorescent dyes, several minutes later. In contrast, the GUVs originally containing V-SM clearly reduced their size as they lost their contents, becoming progressively smaller until suddenly collapsed within the timeframe of a few minutes. Representative movies are provided as the Supporting Information.

SUMMARY AND CONCLUSIONS

This study highlights that when enzymatically generated from the corresponding SMs in comparable experimental conditions, V-Cer has a considerably higher propensity than that of P-Cer of inducing perturbations and structural destabilization in the membranes. Although the increase in levels of any species of Cer is expected to affect the structure of a bilayer,[32] the generation of P-Cer eventually limits, whereas that of V-Cer tends to facilitate the accessibility of the SM substrates originally present in both hemilayers to SMase. The vesicles with decreasing P-SM and increasing P-Cer content maintained in general their monodispersion, size, and shape, whereas their bilayers showed a moderate increase in the lipid order and microviscosity as they increased their permeability gradually. Compared to LUV suspensions initially containing P-SM, in those containing V-SM, the generation of V-Cer resulted in a higher tendency to form large particles and a higher increase in surface structuring and in microviscosity. Moreover, comparing GUVs generating V-Cer and P-Cer, the former displayed a sooner and faster transfer of their contents to the medium along with a decrease in size. Taken together, these results indicate that the V-SM → V-Cer conversion not only results in in-plane but also in transbilayer reordering of lipids that promotes a momentous restructuring of the GUVs' membrane bilayer. The formation of nonplanar structures in the membrane may be in part involved in this rearrangement, which could eventually lead to the observed GUVs to collapse.

The hydrolysis of V-SM shows a rapid initial phase and then a slower phase. The slower part of this curve is consistent with the mentioned lipid reorganization taking place, thereby facilitating access of additional SM molecules to the enzyme for hydrolysis. Such events could promote the translocation (scrambling) of relatively more V-SM than P-SM molecules from the inner to the outer hemilayer during the enzymatic action. This reorganization could respond to the differences observed in lateral intervesicular lipid mixing and membrane recombination, which occurred more efficiently with V-Cer than with P-Cer as SMase lipid products. Combined with the differential increase in lipid order and microviscosity the vesicles displayed, the results suggest that the compositional change involved in the V-SM → V-Cer conversion induces a continuously increasing membrane remodeling that decreases the membrane stability as V-Cer accumulates.

Previous work by Holopainen et al.[33] demonstrated that the generation of P-Cer by *B. cereus* SMase in SOPC/SM GUVs produced vectorial increases of the local curvature of the GUVs' surface. Small vesicles bud to the exterior if the enzyme is injected into GUVs and pouch toward the GUVs' interior to form caveolar-like structures if the enzyme is present in the external medium. These small areas of increased curvature may precede the occurrence of lamellar-to-hexagonal phase transitions. The latter have been shown to lead to the local

DOI: 10.1021/acs.langmuir.7b04374
Langmuir 2018, 34, 4398−4407

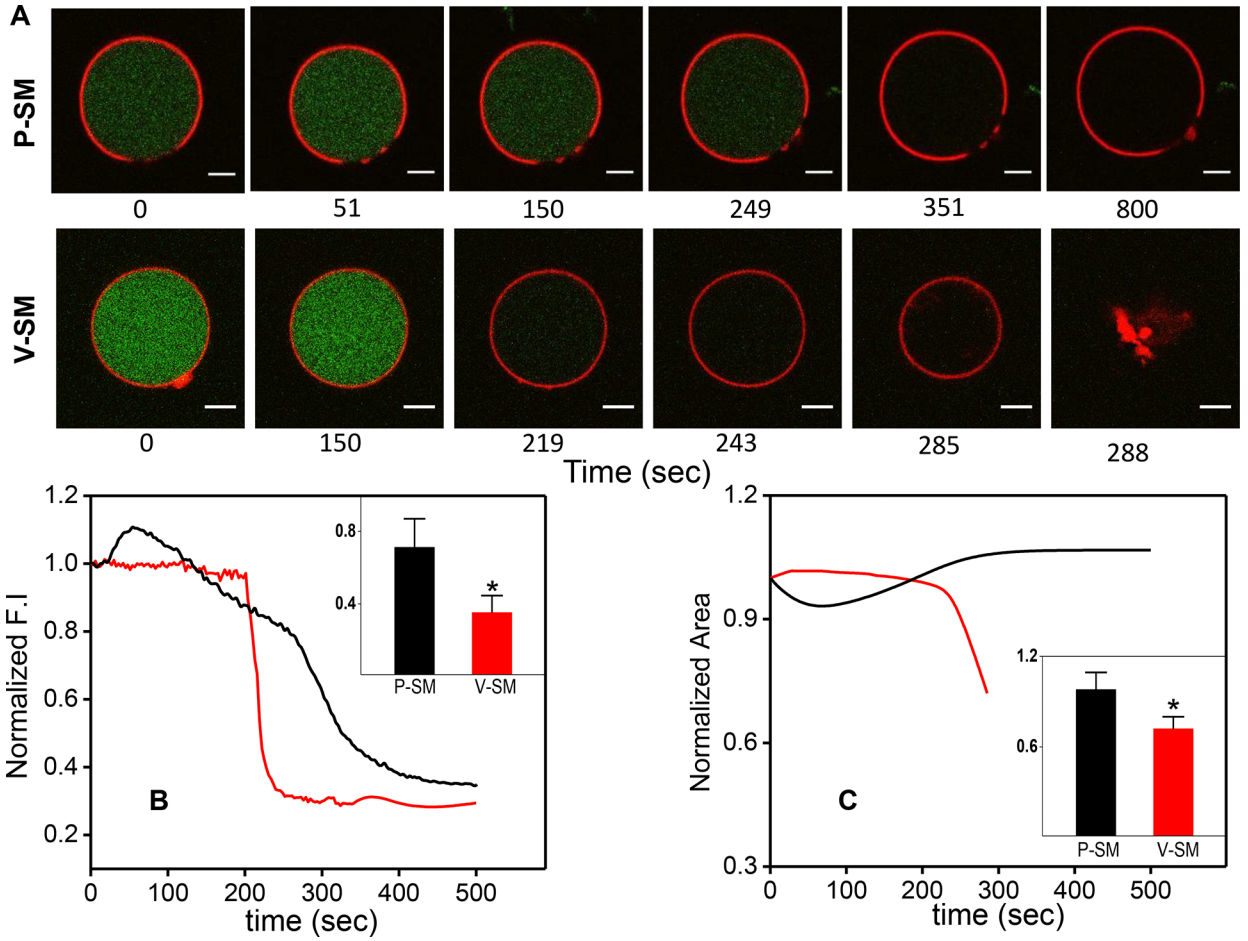

Figure 6. Membrane restructuring after SMase activity. GUVs composed of POPC and either P-SM or V-SM, at 3:1 molar ratios, doubly labeled with a membrane marker (BODIPY-Cer, red) and an inner compartment marker (Alexa^{488}, green), were observed by fluorescence confocal microscopy before (t = 0) and after exposure to SMase at room temperature. (A) Images of a representative experiment taken at the indicated intervals. The scale bar (white lines within images) represents 5 μm. (B) Comparison of the leakage of the green fluorescent content and (C) comparison of the change in GUVs' area (in each case normalized with respect to the corresponding values at t = 0) for GUVs initially containing either P-SM (black lines) or V-SM (red lines). Insets: bars showing the normalized values ± SEM (with n = 4) of fluorescence intensity at t = 240 s in (B) and of the area at t = 280 s in (C). Representative movies sequentially illustrating these changes are provided as Supporting Information Section S1. Magnification of the domains shown for P-SM at t = 0 and for P-Cer at t = 350 s is shown as Supporting Information Section S2.

loss of membrane lipid asymmetry and facilitate translocation (scrambling) of other lipids.[34,35]

In LUVs containing binary mixtures composed of PE and Cer, Sot et al.[36] have explored systematically the modulation of lamellar-to-hexagonal type II phase transitions by Cer species containing different and *N*-acyl chain lengths. The authors showed that in contrast to short-chain species, those with long chains (like P-Cer), because they display an "inverted cone" geometry, favor the negative spontaneous curvature of the membrane outer hemilayer, which facilitates the nonlamellar phase transitions undergone by PE. The present POPC/SM systems lack PE or other hexagonal phase-forming phospholipid while generating cone-shaped Cer species. The fact that the V-Cer species are highly asymmetric in their hydrophobic chains, besides having longer and bulkier fatty acids than those of P-Cer, probably potentiates the conical shape of V-Cer. This allows to hypothesize that at very high V-Cer concentrations, there may be areas of the membrane where such Cer organize in hexagonal type II or even cubic bicontinuous phases. A recent study[37] using a combination of X-ray diffraction techniques and infrared spectroscopy has shown for the first time that another asymmetric Cer species (10:0 Cer), in its pure state, is indeed able to self-organize into a hexagonal lattice.

Summing up, the present study provides direct evidence that the enzymatic generation of V-Cer is an event that promotes dramatic changes in the membrane structure, permeability, and stability and that differ, in nature and in extent, from those induced by the generation of the more "conventional" and ubiquitous species P-Cer. The local adoption of negatively curved structures with the formation of Cer, by promoting transitions of some phospholipid components of the bilayer to nonlamellar phases, has been proposed as intermediate structures in the membrane fusion process.[38] During the acrosomal reaction, fusion events between two bilayers occur at scattered points on the sperm head surface, thereby connecting the plasma membrane and the acrosomal membrane. This fusion is associated with the formation of porelike structures that promote a large increase in permeability, manifested in the release of the enzyme-rich fluid originally secluded within the acrosome. The present membrane models suggest that such, essentially physical, processes can occur faster and more vigorously when V-Cer, rather than P-Cer, is generated from the corresponding SM species. The fact that saturated species

DOI: 10.1021/acs.langmuir.7b04374
Langmuir 2018, 34, 4398−4407

of SM are excluded whereas V-SMs naturally abound on the head of spermatozoa in many mammals may obey the biological advantages provided by these physical characteristics.

■ ASSOCIATED CONTENT

Supporting Information

The Supporting Information is available free of charge on the ACS Publications website at DOI: 10.1021/acs.langmuir.7b04374.

Representative movies comparing the dynamic changes of P-SM (AVI) and V-SM (AVI) depicted in Figure 6 (AVI)(AVI)

Figure legend of representative movies and magnification of the P-SM and P-Cer-enriched domains observed in Figure 6A, showing GUVs composed of POPC and P-SM before (t = 0) and after (t = 350 s) exposure to SMase (PDF)

■ AUTHOR INFORMATION

Corresponding Author

*E-mail: dpenalva@criba.edu.ar. Tel: +54 0291-4861201.

ORCID

Daniel A. Peñalva: 0000-0002-7375-3180

María L. Fanani: 0000-0002-9495-124X

Notes

The authors declare no competing financial interest.

■ ACKNOWLEDGMENTS

This work was supported by funds granted by Consejo Nacional de Investigaciones Científicas y Técnicas (CONICET, PIP112-201101-00843), Agencia Nacional de Promoción de la Ciencia y la Tecnología (ANPCyT, PICT2013-1356 and PICT2014-1627), Universidad Nacional del Sur (UNS, PGI24/B218), and Universidad Nacional de Córdoba (SECyT-UNC366/16). The authors are Career Investigators from CONICET. The microscopy experiments were performed in the Centro de Microscopía Óptica y Confocal Avanzada, Córdoba, Argentina.

■ ABBREVIATIONS

Cer, ceramide; Chol, cholesterol; DLS, dynamic light scattering; DPH, 1,6-diphenyl-1,3,6-hexatriene; FRET, Förster resonance energy transfer; GP, generalized polarization; GUVs, giant unilamellar vesicles; LUVs, large unilamellar vesicles; PE, phosphatidylethanolamine; POPC, 1-palmitoyl-2-oleoyl phosphatidylcholine; P-Cer, palmitate-rich Cer; P-SM, palmitate-rich SM; r, anisotropy; SM, sphingomyelin; SMase, sphingomyelinase; V-Cer, Cer species with VLCPUFA; VLCPUFA, very long-chain polyunsaturated fatty acids; V-SM, sphingomyelin species with VLCPUFA

■ REFERENCES

(1) Poulos, A.; Johnson, D. W.; Beckman, K.; White, I. G.; Easton, C. Occurrence of unusual molecular species of sphingomyelin containing 28-34-carbon polyenoic fatty acids in ram spermatozoa. *Biochem. J.* **1987**, *248*, 961−964.

(2) Furland, N. E.; Zanetti, S. R.; Oresti, G. M.; Maldonado, E. N.; Aveldano, M. I. Ceramides and sphingomyelins with high proportions of very long-chain polyunsaturated fatty acids in mammalian germ cells. *J. Biol. Chem.* **2007**, *282*, 18141−18150.

(3) Robinson, B. S.; Johnson, D. W.; Poulos, A. Novel molecular species of sphingomyelin containing 2-hydroxylated polyenoic very-long-chain fatty acids in mammalian testes and spermatozoa. *J. Biol. Chem.* **1992**, *267*, 1746−1751.

(4) Sandhoff, R.; Geyer, R.; Jennemann, R.; Paret, C.; Kiss, E.; Yamashita, T.; Gorgas, K.; Sijmonsma, T. P.; Iwamori, M.; Finaz, C.; Proia, R. L.; Wiegandt, H.; Grone, H. J. Novel class of glycosphingolipids involved in male fertility. *J. Biol. Chem.* **2005**, *280*, 27310−27318.

(5) Zanetti, S. R.; de Los Angeles, M. M.; Rensetti, D. E.; Fornes, M. W.; Aveldano, M. I. Ceramides with 2-hydroxylated, very long-chain polyenoic fatty acids in rodents: From testis to fertilization-competent spermatozoa. *Biochimie* **2010**, *92*, 1778−1786.

(6) Oresti, G. M.; Reyes, J. G.; Luquez, J. M.; Osses, N.; Furland, N. E.; Aveldano, M. I. Differentiation-related changes in lipid classes with long-chain and very long-chain polyenoic fatty acids in rat spermatogenic cells. *J. Lipid Res.* **2010**, *51*, 2909−2921.

(7) Oresti, G. M.; Luquez, J. M.; Furland, N. E.; Aveldano, M. I. Uneven distribution of ceramides, sphingomyelins and glycerophospholipids between heads and tails of rat spermatozoa. *Lipids* **2011**, *46*, 1081−1090.

(8) Oresti, G. M.; Peñalva, D. A.; Luquez, J. M.; Antollini, S. S.; Aveldaño, M. I. Lipid Biochemical and Biophysical Changes in Rat Spermatozoa During Isolation and Functional Activation In Vitro. *Biol. Reprod.* **2015**, 140.

(9) Peñalva, D. A.; Furland, N. E.; López, G. H.; Aveldaño, M. I.; Antollini, S. S. Unique thermal behavior of sphingomyelin species with nonhydroxy and 2-hydroxy very-long-chain (C28−C32) polyunsaturated fatty acids. *J. Lipid Res.* **2013**, 2225−2235.

(10) Peñalva, D. A.; Oresti, G. M.; Dupuy, F.; Antollini, S. S.; Maggio, B.; Aveldaño, M. I.; Fanani, M. L. Atypical surface behavior of ceramides with nonhydroxy and 2-hydroxy very long-chain (C28−C32) PUFAs. *Biochim. Biophys. Acta* **2014**, *1838*, 731−738.

(11) Goñi, F. M.; Alonso, A. Sphingomyelinases: enzymology and membrane activity. *FEBS Lett.* **2002**, *531*, 38−46.

(12) Goñi, F. M.; Alonso, A. Biophysics of sphingolipids I. Membrane properties of sphingosine, ceramides and other simple sphingolipids. *Biochim. Biophys. Acta* **2006**, *1758*, 1902−1921.

(13) Castro, B. M.; Prieto, M.; Silva, L. C. Ceramide: a simple sphingolipid with unique biophysical properties. *Prog. Lipid Res.* **2014**, *54*, 53−67.

(14) Silva, L. C.; Futerman, A. H.; Prieto, M. Lipid raft composition modulates sphingomyelinase activity and ceramide-induced membrane physical alterations. *Biophys. J.* **2009**, *96*, 3210−3222.

(15) López-Montero, I.; Vélez, M.; Devaux, P. F. Surface tension induced by sphingomyelin to ceramide conversion in lipid membranes. *Biochim. Biophys. Acta* **2007**, *1768*, 553−561.

(16) Montes, L. R.; Ruiz-Arguello, M. B.; Goñi, F. M.; Alonso, A. Membrane restructuring via ceramide results in enhanced solute efflux. *J. Biol. Chem.* **2002**, *277*, 11788−11794.

(17) Parasassi, T.; Loiero, M.; Raimondi, M.; Ravagnan, G.; Gratton, E. Absence of lipid gel-phase domains in seven mammalian cell lines and in four primary cell types. *Biochim. Biophys. Acta* **1993**, *1153*, 143−154.

(18) Shinitzky, M.; Yuli, I. Lipid fluidity at the submacroscopic level: Determination by fluorescence polarization. *Chem. Phys. Lipids* **1982**, *30*, 261−282.

(19) Maggio, B.; Yu, R. K. Interaction and fusion of unilamellar vesicles containing cerebrosides and sulfatides induced by myelin basic protein. *Chem. Phys. Lipids* **1989**, *51*, 127−36.

(20) Angelova, M. I.; Soléau, P.; Méléard, J.; Faucon, F.; Bothorel, P. Preparation of giant vesicles by external AC electric fields. Kinetics and applications. *Prog. Colloid Polym. Sci.* **1992**, *89*, 127−131.

(21) Ambroggio, E. E.; Separovic, F.; Bowie, J. H.; Fidelio, G. D.; Bagatolli, L. A. Direct visualization of membrane leakage induced by the antibiotic peptides: maculatin, citropin, and aurein. *Biophys. J.* **2005**, *89*, 1874−1881.

(22) Ruiz-Argüello, M. B.; Veiga, M. P.; Arrondo, J. L.; Goñi, F. M.; Alonso, A. Sphingomyelinase cleavage of sphingomyelin in pure and mixed lipid membranes. Influence of the physical state of the sphingolipid. *Chem. Phys. Lipids* **2002**, *114*, 11−20.

DOI: 10.1021/acs.langmuir.7b04374
Langmuir 2018, 34, 4398−4407

(23) de Almeida, R. F.; Fedorov, A.; Prieto, M. Sphingomyelin/phosphatidylcholine/cholesterol phase diagram: boundaries and composition of lipid rafts. *Biophys. J.* **2003**, *85*, 2406−2416.
(24) Bagatolli, L. A.; Maggio, B.; Aguilar, F.; Sotomayor, C. P.; Fidelio, G. D. Laurdan properties in glycosphingolipid-phospholipid mixtures: a comparative fluorescence and calorimetric study. *Biochim. Biophys. Acta* **1997**, *1325*, 80−90.
(25) Parasassi, T.; De, S. G.; d'Ubaldo, A.; Gratton, E. Phase fluctuation in phospholipid membranes revealed by Laurdan fluorescence. *Biophys. J.* **1990**, *57*, 1179−1186.
(26) Lakowicz, J. et al. Fluorescence Anisotropy. In *Principles of Fluorescence Spectroscopy*; Plenum Publishers: New York, 1999; pp 291−319.
(27) Holopainen, J. M.; Subramanian, M.; Kinnunen, P. K. Sphingomyelinase induces lipid microdomain formation in a fluid phosphatidylcholine/sphingomyelin membrane. *Biochemistry* **1998**, *37*, 17562−17570.
(28) Silva, L.; de Almeida, R. F.; Fedorov, A.; Matos, A. P.; Prieto, M. Ceramide-platform formation and -induced biophysical changes in a fluid phospholipid membrane. *Mol. Membr. Biol.* **2006**, *23*, 137−148.
(29) Castro, B. M.; de Almeida, R. F.; Silva, L. C.; Fedorov, A.; Prieto, M. Formation of ceramide/sphingomyelin gel domains in the presence of an unsaturated phospholipid: a quantitative multiprobe approach. *Biophys. J.* **2007**, *93*, 1639−1650.
(30) Peñalva, D. A.; Wilke, N.; Maggio, B.; Aveldaño, M. I.; Fanani, M. L. Surface behavior of sphingomyelins with very long chain polyunsaturated Fatty acids and effects of their conversion to ceramides. *Langmuir* **2014**, *30*, 4385−4395.
(31) Fanani, M. L.; Hartel, S.; Maggio, B.; De, T. L.; Jara, J.; Olmos, F.; Oliveira, R. G. The action of sphingomyelinase in lipid monolayers as revealed by microscopic image analysis. *Biochim. Biophys. Acta* **2010**, *1798*, 1309−1323.
(32) Pinto, S. N.; Silva, L. C.; Futerman, A. H.; Prieto, M. Effect of ceramide structure on membrane biophysical properties: the role of acyl chain length and unsaturation. *Biochim. Biophys. Acta* **2011**, *1808*, 2753−2760.
(33) Holopainen, J. M.; Angelova, M. I.; Kinnunen, P. K. Vectorial budding of vesicles by asymmetrical enzymatic formation of ceramide in giant liposomes. *Biophys. J.* **2000**, *78*, 830−838.
(34) Tepper, A. D.; Ruurs, P.; Wiedmer, T.; Sims, P. J.; Borst, J.; van Blitterswijk, W. J. Sphingomyelin hydrolysis to ceramide during the execution phase of apoptosis results from phospholipid scrambling and alters cell-surface morphology. *J. Cell Biol.* **2000**, *150*, 155−164.
(35) Contreras, F. X.; Villar, A. V.; Alonso, A.; Kolesnick, R. N.; Goñi, F. M. Sphingomyelinase activity causes transbilayer lipid translocation in model and cell membranes. *J. Biol. Chem.* **2003**, *278*, 37169−37174.
(36) Sot, J.; Aranda, F. J.; Collado, M. I.; Goñi, F. M.; Alonso, A. Different effects of long- and short-chain ceramides on the gel-fluid and lamellar-hexagonal transitions of phospholipids: a calorimetric, NMR, and X-ray diffraction study. *Biophys. J.** **2005**, *88*, 3368−3380.
(37) Dupuy, F. G.; Fernández Bordín, S. P.; Maggio, B.; Oliveira, R. G. Hexagonal phase with ordered acyl chains formed by a short chain asymmetric ceramide. *Colloids Surf., B* **2017**, *149*, 89−96.
(38) Seddon, J. M. Structure of the inverted hexagonal (HII) phase, and non-lamellar phase transitions of lipids. *Biochim. Biophys. Acta* **1990**, *1031*, 1−69.

DOI: 10.1021/acs.langmuir.7b04374
Langmuir 2018, 34, 4398−4407